Cellular and Molecular Life Sciences (2022) 79:355
https://doi.org/10.1007/s00018-022-04328-9

Cellular and Molecular Life Sciences

ORIGINAL ARTICLE

Recirculating Foxp3$^+$ regulatory T cells are restimulated in the thymus under Aire control

Jonathan Charaix[1] · Alexia Borelli[1] · Jérémy C. Santamaria[1] · Lionel Chasson[1] · Matthieu Giraud[2] · Arnauld Sergé[3] · Magali Irla[1]

Received: 14 January 2022 / Revised: 13 April 2022 / Accepted: 26 April 2022 / Published online: 9 June 2022
© The Author(s), under exclusive licence to Springer Nature Switzerland AG 2022

Abstract

Thymically-derived Foxp3$^+$ regulatory T cells (T$_{reg}$) critically control immunological tolerance. These cells are generated in the medulla through high affinity interactions with medullary thymic epithelial cells (mTEC) expressing the Autoimmune regulator (Aire). Recent advances have revealed that thymic T$_{reg}$ contain not only developing but also recirculating cells from the periphery. Although Aire is implicated in the generation of Foxp3$^+$ T$_{reg}$, its role in the biology of recirculating T$_{reg}$ remains elusive. Here, we show that Aire regulates the suppressive signature of recirculating T$_{reg}$ independently of the remodeling of the medullary 3D organization throughout life where T$_{reg}$ reside. Accordingly, the adoptive transfer of peripheral Foxp3$^+$ T$_{reg}$ in *Aire*^{KO} recipients led to an impaired suppressive signature upon their entry into the thymus. Furthermore, recirculating T$_{reg}$ from *Aire*^{KO} mice failed to attenuate the severity of multiorgan autoimmunity, demonstrating that their suppressive function is altered. Using bone marrow chimeras, we reveal that mTEC-specific expression of Aire controls the suppressive signature of recirculating T$_{reg}$. Finally, mature mTEC lacking *Aire* were inefficient in stimulating peripheral T$_{reg}$ both in polyclonal and antigen-specific co-culture assays. Overall, this study demonstrates that Aire confers to mTEC the ability to restimulate recirculating T$_{reg}$, unravelling a novel function for this master regulator in T$_{reg}$ biology.

Keywords Autoimmune regulator · Autoimmunity · Medullary thymic epithelial cells · Foxp3$^+$ regulatory T cells · Thymus

Introduction

CD25$^+$Foxp3$^+$ regulatory T cells (T$_{reg}$) constitute a distinct subset of CD4$^+$ T cells endowed with suppressive functions. By maintaining immune tolerance, T$_{reg}$ critically prevent the emergence of autoimmune and inflammatory diseases. The vast majority of T$_{reg}$ is produced in the thymic medulla where they arise from two distinct developmental programs involving CD25$^+$Foxp3$^-$ (CD25$^+$ T$_{reg}$P) and CD25$^-$Foxp3^{lo} (Foxp3^{lo} T$_{reg}$P) precursors [1–4]. For a long-time, thymic CD25$^+$Foxp3$^+$ T$_{reg}$ were thought to exclusively correspond to developing cells. However, recent studies have shown that circulating CD25$^+$Foxp3$^+$ T$_{reg}$ have the ability to migrate back into the thymus [5–7]. Thus, thymic CD25$^+$Foxp3$^+$ T$_{reg}$ is a heterogeneous population containing both developing and recirculating cells [3]. Interestingly, recirculating T$_{reg}$ show suppressive properties similar to their splenic counterparts [7]. They exhibit an activated and differentiated phenotype and were found to negatively regulate the de novo generation of CD25$^+$Foxp3$^+$ T$_{reg}$ through IL-2 consumption [5].

The recirculation of peripheral Foxp3$^+$ T$_{reg}$ in the thymus is mediated at least by two chemokine receptors, CCR6 and CXCR4 [5, 8]. Interestingly, the entry of peripheral *Ccr6*$^{-/-}$ T$_{reg}$ into the thymus is impaired, suggesting that CCR6, expressed by effector/memory T cells, is involved in the recirculation of Foxp3$^+$ T$_{reg}$ from the periphery to this organ [8]. Furthermore, the expression of the CCR6 ligand, CCL20, is regulated by the Autoimmune regulator (Aire) [8].

Jonathan Charaix, Alexia Borelli have contributed equally to this work.

✉ Magali Irla
Magali.Irla@inserm.fr

[1] Centre d'Immunologie de Marseille-Luminy, Aix-Marseille University, CNRS, INSERM, CIML, Marseille, France

[2] Center for Research in Transplantation and Translational Immunology, UMR 1064, INSERM, Nantes Université, 44000 Nantes, France

[3] Turing Centre for Living Systems, Laboratoire adhésion inflammation (LAI), CNRS, INSERM, Aix-Marseille University, 13288 Marseille, France

Aire is mainly expressed by a subset of medullary thymic epithelial cells (mTEC) commonly called $mTEC^{hi}$, characterized by a $CD80^{hi}MHCII^{hi}$ phenotype. Furthermore, upon recirculation into the thymus, a subset of B cells has been described to upregulate Aire [9]. Independent reports have described that $CD25^{+}Foxp3^{+}$ T_{reg} are reduced in the thymus of *Aire*^{KO} mice [10, 11]. Accordingly, *Aire* expression was proposed to direct autoreactive $CD4^{+}$ thymocytes into the T_{reg} cell lineage [12]. Interestingly, in the perinatal life, Aire promotes the generation of a distinct population of $Foxp3^{+}$ T_{reg}, which persists in adults and prevents the emergence of autoimmunity [13]. In C57BL/6 mice, *Aire*-deficiency is associated with mild autoimmunity characterized by lymphocyte infiltrations and autoantibody production targeting several organs such as the pancreas, eyes, salivary glands, liver and lungs [14–17]. In human, autosomal recessive mutations in the *Aire* gene induce a life-threatening pathology called autoimmune polyendocrinopathy–candidiasis–ectodermal dystrophy (APECED), also known as autoimmune polyendocrine syndrome-type 1 (APS-1) [18, 19]. Interestingly, numbers, activation and suppressive functions of $Foxp3^{+}$ T_{reg} are altered in APECED patients [20–22].

Although thymic $Foxp3^{+}$ T_{reg} have been found to be more heterogeneous than previously thought [3], this emerging population of recirculating peripheral T_{reg} remains poorly described. In particular, the mechanisms that control their suppressive phenotype in the thymus are unknown. In this study, we show that Aire regulates the suppressive properties of recirculating $CCR6^{+}$ T_{reg}, independently of the remodeling of the 3D organization of the thymic medulla where they reside [5]. High-throughput sequencing revealed that recirculating $CCR6^{+}$ T_{reg} in the thymus of *Aire*^{KO} mice have impaired expression of several genes associated with T_{reg} suppressive functions and helper T cell polarization. Accordingly, recirculating $CCR6^{+}$ T_{reg} from *Aire*^{KO} mice failed to attenuate the severity of multiorgan autoimmunity, demonstrating that their suppressive activity is impaired. Moreover, the adoptive transfer of splenic $Foxp3^{+}$ T_{reg} in *Aire*^{KO} recipients resulted in an impaired suppressive signature upon their recirculation in the thymus. Using bone marrow (BM) chimeras, we demonstrate that *Aire* expressed by mTEC rather than by thymic B cells is responsible for the suppressive properties of recirculating $CCR6^{+}$ T_{reg}. Finally, recirculating T_{reg} were found in close contact with $Aire^{+}$ mTEC and restimulated in an antigen-specific manner. Altogether, our data reveal that Aire confers to mTEC the capacity to control the restimulation of recirculating $CCR6^{+}$ T_{reg} in the thymus.

Materials and methods

Mice

CD45.1 WT (B6.SJL-*PtprcaPepcb*/BoyCrl, Stock n°002,014, Charles River), CD45.2 WT (Stock n°000,664, Charles River), CD45.1/2 WT, CD45.2 *Aire*^{KO} [23], *Rag2*^{KO} [24], CD45.1 $Foxp3^{eGFP}$ mice [25], OTII [26] and Rip-mOVA [27] were on a C57BL/6 J background. Rip-mOVA × OTII mice were backcrossed on a *Rag2*^{KO} background. All mice were maintained under specific pathogen-free conditions at the Centre d'Immunologie de Marseille–Luminy (CIML, France). Standard food and water were given ad libitum. Males and females were used at the age of 5 days, 9 days, 6 weeks and 1 year. Chimeras were generated between 6 and 10 weeks of age. All experiments were done in accordance with National and European laws for laboratory animal welfare (EEC Council Directive 2010/63/UE) and the Marseille Ethical Committee for Animal experimentation no. 14.

BM chimeras

BM chimeras were generated by injecting intravenously (*i.v.*) 5.10^{6} BM cells from CD45.1 $Foxp3^{eGFP}$ mice into lethally irradiated CD45.2 *Aire*^{WT} or *Aire*^{KO} recipients (two doses of 500 rads, 8 h apart, X-ray using a RS-2 000 Irradiator; Rad Source Technologies). Similarly, 5.10^{6} BM cells from either CD45.2 *Aire*^{WT} or *Aire*^{KO} mice were injected into lethally irradiated CD45.1/2 WT recipients. Mice were analyzed 6-weeks post-reconstitution.

$Foxp3^{+}$ T_{reg} adoptive transfer

5.10^{5} cell-sorted splenic congenic CD45.1 $CD4^{+}CD25^{+}Foxp3^{eGFP}$ T_{reg} were *i.v* injected into sublethally irradiated CD45.2 *Aire*^{WT} or *Aire*^{KO} recipient mice (one dose of 500 rads, X-ray using a RS-2 000 Irradiator; Rad Source Technologies). Mice were analyzed 1-week post-T_{reg} adoptive transfer.

Multiorgan autoimmunity experiments

Rag2^{KO} recipients were injected *i.v.* with 3.10^{6} $CD4^{+}CD25^{+}$ T_{reg}-depleted splenocytes purified from CD45.1 WT mice. Four weeks later, 15.10^{4} splenic $CD4^{+}CD25^{hi}$ T_{reg} or 10.10^{4} recirculating thymic $CCR6^{+}CD4^{+}CD25^{+}$ T_{reg} from *Aire*^{WT} or *Aire*^{KO} mice were adoptively transferred. Mice that did not receive any T_{reg} were used as controls. Peripheral tissues were harvested and analyzed three weeks later.

Cell isolation

Thymic T_{reg}, splenic T_{reg} and T_{reg}-depleted splenocytes were isolated by scratching the thymus or the spleen on a 70-µm mesh. Red blood cells were lysed with RBC lysis buffer (eBioscience). Thymic and splenic T_{reg} cells were pre-enriched by depleting CD8^{+} and CD19^{+} cells using biotinylated anti-CD8α (clone 53.6.7; BD Biosciences) and anti-CD19 (clone 1D3; BD Biosciences) antibodies with antibiotin microbeads by AutoMACS using the Deplete program (Miltenyi Biotec). Recirculating thymic T_{reg} were sorted as CCR6^{+}CD4^{+}CD8^{-}CD25^{+} cells and splenic T_{reg} as CD4^{+}CD25^{hi} cells using a FACSAria III cell sorter (BD Biosciences). Splenocytes were depleted of CD4^{+}CD25^{+} T_{reg} using a FACSAria III cell sorter (BD Biosciences). Thymus were digested at 37 °C in HBSS medium containing Liberase TM (50 µg/ml; Roche) and DNase I (100 µg/ml; Roche) until complete tissue digestion. Total mTEC (CD45^{-}EpCAM^{+}UEA-1^{+}Ly51$^{-/lo}$) or mTEC^{hi} (CD45^{-}EpCAM^{+}UEA-1^{+}Ly51$^{-/lo}$CD80^{hi}) were pre-enriched by depleting CD45 hematopoietic cells using anti-CD45 magnetic beads (Miltenyi Biotec) by AutoMACS with the DepleteS program and sorted using a FACSAria III cell sorter (BD Biosciences).

In vitro co-culture assays

3.10^{4} cell-sorted splenic CD4^{+}CD25^{hi} T_{reg} from *Aire*^{WT} or *Aire*^{KO} mice were co-cultured for 24 h with 6.10^{3} CD45^{-}EpCAM^{+}UEA-1^{+}Ly51$^{-/lo}$ mTEC from *Aire*^{WT} or *Aire*^{KO} mice in RPMI (ThermoFisher) supplemented with 10% FBS (Sigma Aldrich), L-glutamine (2 mM, ThermoFisher), sodium pyruvate (1 mM, ThermoFisher), 2-mercaptoethanol (2×10^{-5} M, ThermoFisher), penicillin (100 IU/ml, ThermoFisher), streptomycin (100 µg / ml, ThermoFisher) and mouse IL-2 (40 ng/ml, Immunotools). For antigen-specific co-culture assays, 5.10^{3} cell-sorted splenic CD4^{+}CD25^{hi} T_{reg} from Rip-mOVA x OTII x *Rag2*^{KO} mice were co-cultured for 24 h with 1.10^{3} CD45^{-}EpCAM^{+}Ly51$^{-/lo}$Aire^{eGFP} mTEC from *Aire*^{het} or *Aire*^{KO} mice previously loaded with $OVA_{323-339}$ peptide (5 µg/ml, Polypeptide group) for 2 h.

Flow cytometry

Cells were stained with standard procedures using antibodies listed in Table S2. For intracellular staining with anti-Foxp3, anti-GITRL and anti-OX40L antibodies, cells were fixed, permeabilized and stained with the Foxp3 staining kit according to the manufacturer's instructions (eBioscience). Stained cells were analyzed with FACSCanto II and LSR II (BD Biosciences) and data were analyzed using FlowJo software (Tree Star).

Quantitative RT-PCR

The total RNA was extracted with TRIzol (Invitrogen) and cDNA was synthesized with random oligo dT primers and Superscript II reverse transcriptase (Invitrogen). Quantitative PCR was performed with SYBR Premix Ex Taq Master Mix (Takara) on an ABI 7500 fast real-time PCR system (Applied Biosystem). The results were normalized to actin mRNA expression. A list of primer sequences is provided in Table S3.

RNA-sequencing experiments

5.10^{4} CCR6^{+} T_{reg} were cell-sorted from the thymus of 6-week-old *Aire*^{WT} and *Aire*^{KO} mice. Two biological replicates were prepared for each condition. The total RNA was extracted using the RNeasy Micro Kit (Qiagen) and treated with DNase I. RNA-seq libraries were prepared using the TruSeq Stranded mRNA kit (Illumina) and sequenced with the Illumina HiSeq 2000 machine to generate datasets of single-end 50 bp reads. The reads were mapped to the mouse reference genome (mm10) using TopHat2 (version 2.0.12) [28], then counted using Cufflinks or Cuffdiff (version 2.2.1) [29, 30] and the mm10 genome GTF gene annotation file. In addition to read counting, Cuffdiff performs between-sample normalization and was used to calculate the differential gene expression and its statistical significance in *Aire*^{WT} vs *Aire*^{KO} T_{reg} by using the default "pooled" dispersion method that applies to experiments having few (≥ 2) biological replicates per condition. Expression levels generated by Cufflinks, as fragments per kilobase of transcript per million mapped reads (FPKM), were processed by the Matrix2png program [31] to generate heatmaps of gene expression levels. The dataset generated in this study are available in the Gene Expression Omnibus (GEO) database under accession number GSE188419. The expression of *Tnfsf4* and *Tnfsf18* was analyzed in RNA-sequencing dataset from *Aire*^{KO} mTEC^{hi} (GSE87133).

Immunofluorescence staining

Thymi were collected from 9-day-, 6-week- and 1-year-old *Aire*^{WT} or *Aire*^{KO} mice and fat tissues removed to avoid any interference with the 3D reconstitution process. Organs were longitudinally included in O.C.T (Sakura Finetek), frozen at -80 °C and cut in 20-µm-thick slices. Thymic sections were fixed with 2% paraformaldehyde, then saturated with 3% BSA and 0.01% Triton X100 in 0.1 M Tris HCl buffer. Sections were next stained for 45 min with rabbit anti-keratin 14 or with anti-Aire Alexa Fluor 488 (5H12; eBioscience), anti-Foxp3 PE (FJK-16 s; eBioscience) and anti-CD73 Alexa Fluor 647 (TY/11.8; BioLegend) in hybridization buffer (1% BSA and 0.02% Triton X100 in 0.1 M Tris–HCl, pH 7.4). Keratin 14 staining was revealed with Cy3-conjugated anti-rabbit

(Invitrogen). Sections were counterstained with DAPI (1 µL/ml, BioLegend) and mounted with Mowiol (Calbiochem). For 3D reconstruction, images were acquired with a slide scanner (Panoramic SCAN II; 3D Histech). Confocal microscopy was performed with a LSM 780 confocal microscope (Carl Zeiss Microscopy).

Detection of immune infiltrates and autoantibodies

Peripheral tissues were fixed in buffered 10% formalin solution. 4 µm-thick paraffin-embedded sections were counterstained with hematoxylin and eosin. Autoantibody production was assessed by immunostaining organ sections from *Rag2*^{KO} mice with the sera (1/80) of analyzed mice. Autoantibodies were revealed with FITC-conjugated goat anti-mouse IgG. Sections were counterstained with DAPI and mounted with Mowiol (Calbiochem). All images were acquired with a slide scanner (Panoramic SCAN II; 3D Histech) and analyzed with ImageJ software (National Institutes of Health) to compute the mean fluorescence intensity of each image.

Thymic 3D reconstitution

For 3D reconstitution, images from the entire thymus of 9-day-, 6-week- and 1-year-old *Aire*^{WT} and *Aire*^{KO} mice were processed with For3D software as previously described [32, 33]. Briefly, images were smoothed by median and Gaussian filtering and medulla volumes were determined using ImageJ and Matlab (The Mathworks) software. Medullary islets identified in the 3D structures were measured individually using ImageJ and were color-coded using Imaris (Bitplane).

Statistical analysis

Statistics were performed with GraphPad Prism 9.1 software. Normal distribution of the data was assessed using d'Agostino–Pearson omnibus normality test. Statistical significance was then assessed using unpaired Student's *t* test for two normal distributions, Mann–Whitney test for two non-normal distributions or Kruskal–Wallis test for more than two distributions. $*p<0.05$; $**p<0.01$; $***p<0.001$, $****p<0.0001$. All bar graphs show mean ± SEM, unless mentioned.

Results

Aire regulates the recirculation of peripheral CD25$^+$Foxp3$^+$ T$_{reg}$ in the thymus, independently of the remodeling of the 3D organization of the medulla throughout life

Considering the importance of Aire in the induction of self-tolerance [34], we first assessed whether it could be involved in the topology of the thymic medulla. For this, we compared WT (*Aire*^{WT} mice) with *Aire*-deficient mice in which the first exon of the *Aire* locus was replaced by the sequence of enhanced green fluorescent protein (eGFP) (*Aire*^{KO} mice) [23]. Thymic sections of 9-day-, 6-week- and 1-year-old, either from *Aire*^{WT} or *Aire*^{KO} mice, were stained with the keratin-14 mTEC-specific marker [35] and reconstructed with our in-house dedicated "Full organ reconstruction in 3D" (For3D) software [33] (Fig. 1A–C and Movies S1–6). Interestingly, the number of medullary islets in *Aire*^{WT} mice diminished between 9 days and 6 weeks of age while it increased between 6 weeks and 1 year of age (Fig. 1D). Furthermore, the total and individual medullary volumes increased between 9 days and 6 weeks while it decreased between 6 weeks and 1 year (Fig. 1E, F). Nevertheless, the central compartment of ~ 1 mm^3 was observed at all ages analyzed (Fig. 1F) These observations reveal that the medulla organization is dynamic throughout life. In comparison to *Aire*^{WT} mice, the thymi of *Aire*^{KO} mice show a similar dynamic medulla organization characterized by normal numbers of medullary islets and total medullary volumes with the presence of a major compartment (Fig. 1A–C, F). These results indicate that the dynamic remodeling of the 3D organization of the thymic medulla throughout life is not regulated by Aire.

Because medulla formation correlates with Foxp3$^+$ T$_{reg}$ emergence during ontogeny [36], we next analyzed whether *Aire* deficiency could affect their development in neonates of 5 days of age. In contrast to CD25$^+$ T$_{reg}$P, frequencies and numbers of Foxp3^{lo} T$_{reg}$P and mature CD25$^+$Foxp3$^+$ T$_{reg}$ were diminished in the thymus of 5-day-old *Aire*^{KO} mice as compared to their respective counterparts (Fig. 2A). This decrease was also observed in 6-week- and 1-year-old *Aire*^{KO} mice (Fig. 2B, C). Since mature CD25$^+$Foxp3$^+$ T$_{reg}$ contain both developing and recirculating cells in the adult thymus, we used the key thymus-homing chemokine receptor CCR6 to distinguish developing (CCR6$^-$) and recirculating (CCR6$^+$) mature T$_{reg}$ [6]. Interestingly, both numbers of CCR6$^-$ and CCR6$^+$ mature T$_{reg}$ were reduced in *Aire*^{KO} mice compared to *Aire*^{WT} mice at 6 weeks and 1 year of age (Fig. 2D, E). Furthermore, 1-year-old *Aire*^{WT} mice showed a marked

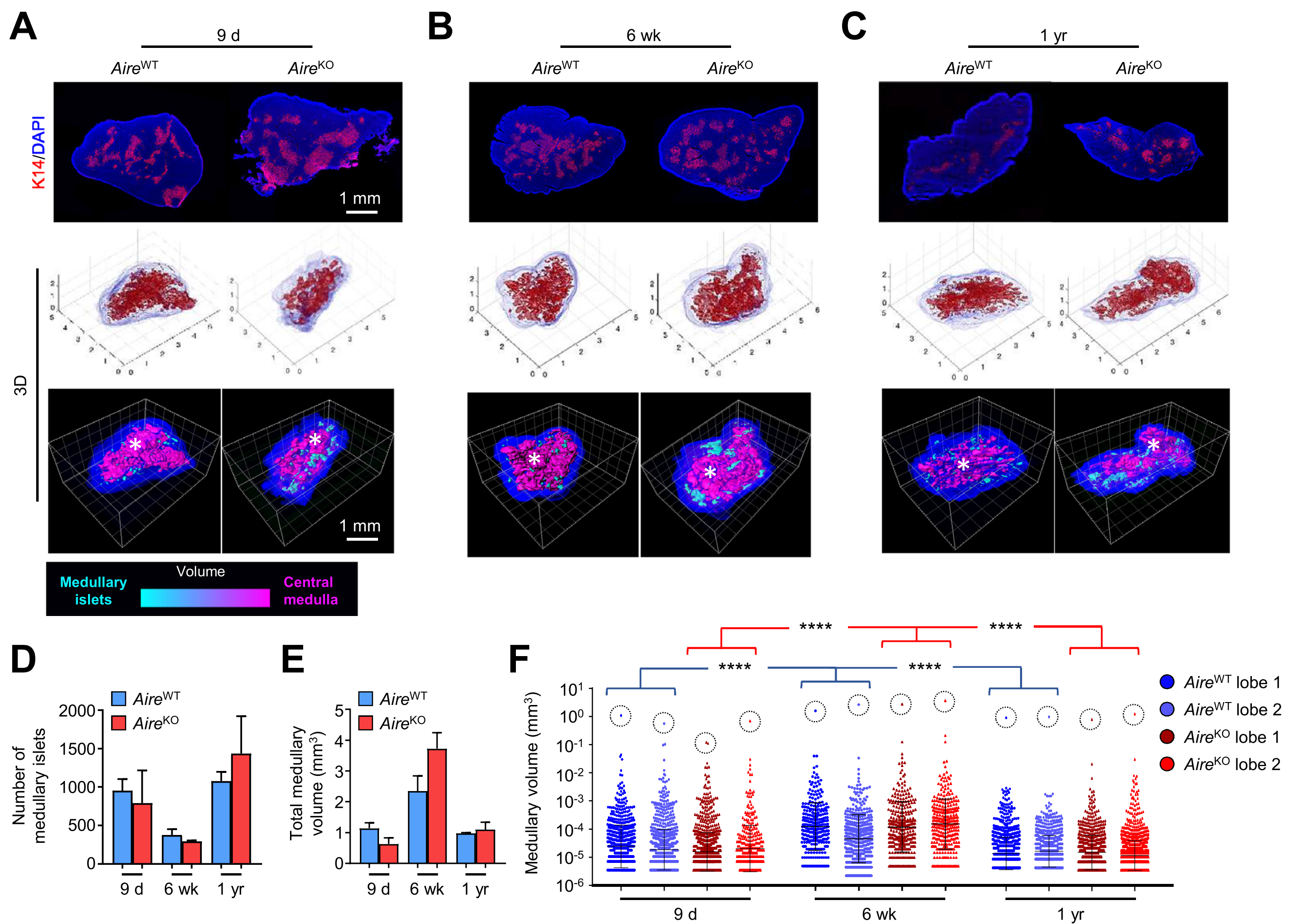

Fig. 1 The medullary topology is dynamic throughout life, independently of *Aire* expression. **A–C** Representative images of thymic sections stained for keratin 14 (red) and counterstained with DAPI (blue) (upper panel). For3D reconstruction of thymic lobes from 9-day- (**A**), 6-week- (**B**) and 1-year-old (**C**) $Aire^{WT}$ and $Aire^{KO}$ mice, using Matlab (middle panel) and Imaris to depict medullary regions according to their volumes from cyan (smallest) to magenta (largest) (lower panel). Axes are graduated in millimeters (mm). Scale bar, 1 mm. The asterisk denotes the central medulla. **D,E** Histograms show the number of medullary islets (**D**) and the total medullary volume (**E**) derived from two thymic lobes for each condition. **F** The graph shows the volumes of each medullary islet derived from two thymic lobes for each condition from individual mice measured by For3D. The dashed circle denotes the central medulla of each lobe. Horizontal lines represent the geometric mean and SD. ****$p < 0.0001$ using Kruskal–Wallis test for (**F**)

reduction in numbers of $CCR6^-$ and $CCR6^+$ mature $CD25^+Foxp3^+$ T_{reg} as compared to 6-week-old $Aire^{WT}$ mice, which reflects the effect of thymic involution on T_{reg} cells in normal conditions. To date, two chemokine receptors, CCR6 and CXCR4 have been implicated in the recirculation of peripheral T_{reg} into the thymus [5, 8]. Strikingly, the expression of their respective ligands, *Ccl20* and *Cxcl12*, was substantially reduced in $Aire^{KO}$ $mTEC^{hi}$ (Fig. 2F), consistently with the altered recirculation of peripheral T_{reg} in the thymus. Altogether, these results show that Aire controls both the development and recirculation of $Foxp3^+$ T_{reg} throughout life.

Thymic $CCR6^+$ T_{reg} from $Aire^{KO}$ mice show an impaired effector and suppressive phenotype

Because Aire controls the recirculation of $CCR6^+$ T_{reg}, we made the hypothesis that it could also control their suppressive properties. To test this hypothesis, we first measured the expression level of several genes associated with T_{reg} suppressive functions in purified $CCR6^+CD4^+CD25^+$ single-positive (SP) thymocytes that correspond to $CD25^+Foxp3^+$ T_{reg} (Fig. S1). Interestingly, whereas *Foxp3* level was normal, the expression of *Klrg1*, a marker of terminally differentiated T_{reg} [37], was reduced in $CCR6^+$ T_{reg} from 6-week-old $Aire^{KO}$ mice (Fig. 3A). Accordingly, the expression of genes encoding for the inhibitory cytokine *Il10*, the cytolytic molecules *Gzmb* and *Fasl*, *Lag3*-associated with dendritic

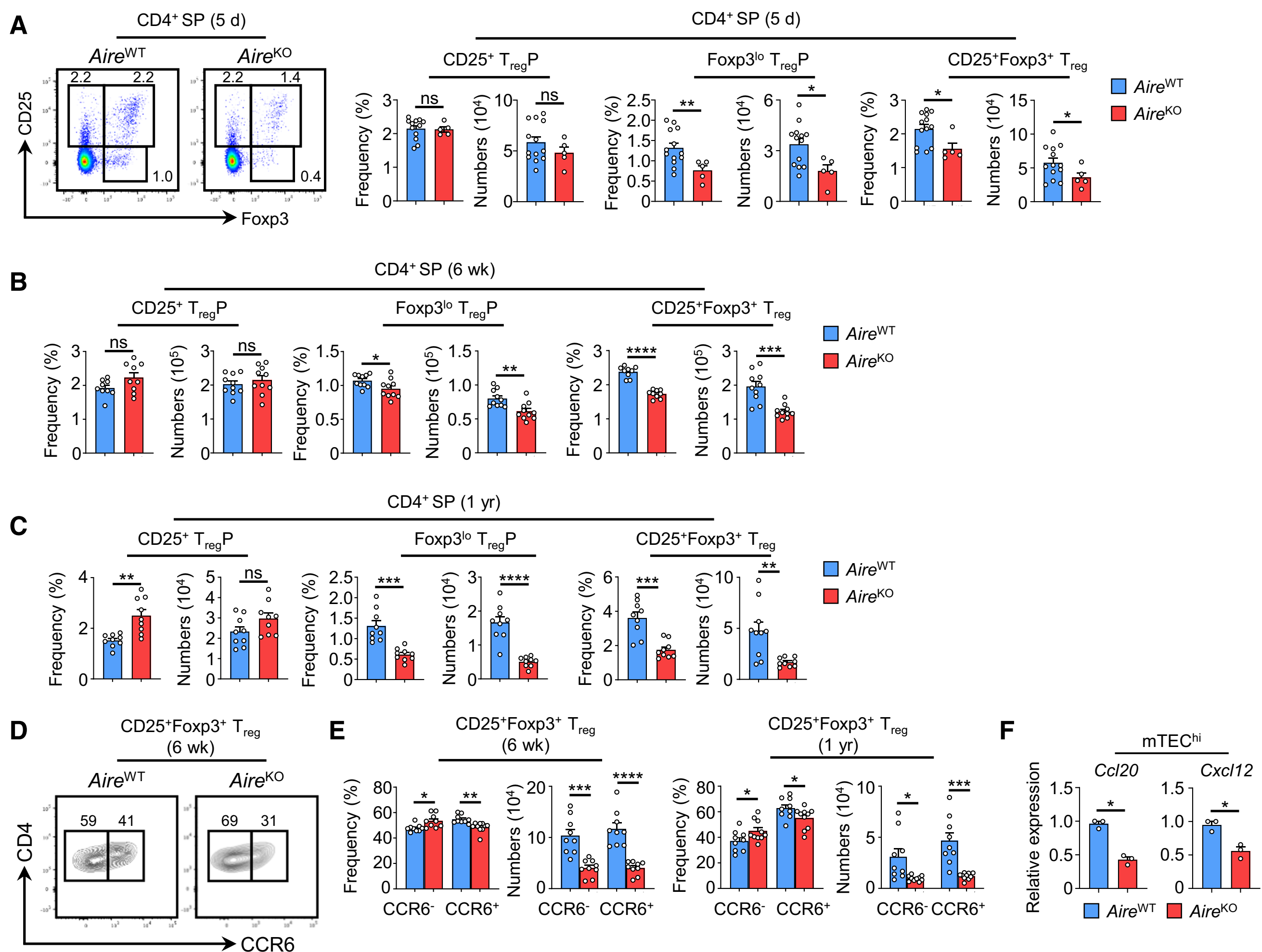

Fig. 2 Developing CCR6⁻ and recirculating CCR6⁺ T_{reg} are reduced in *Aire*^{KO} mice throughout life. **A** Flow cytometry profiles, frequencies and numbers of CD25⁺ T_{reg}P, Foxp3^{lo} T_{reg}P and CD25⁺Foxp3⁺ T_{reg} analyzed in CD4⁺ SP thymocytes from the thymus of 5-day-old *Aire*^{WT} and *Aire*^{KO} mice. The data are derived from 3 independent experiments (n = 2–4 mice per group and per experiment). **B**, **C** Frequencies and numbers of CD25⁺ T_{reg}P, Foxp3^{lo} T_{reg}P and CD25⁺Foxp3⁺ T_{reg} in the thymus of 6-week- (**B**) and 1-year- (**C**) old *Aire*^{WT} and *Aire*^{KO} mice. **D**, **E** Flow cytometry profiles (**D**), frequencies and numbers (**E**) of CCR6⁻ and CCR6⁺ cells in CD25⁺Foxp3⁺ T_{reg} from 6-week- and 1-year-old *Aire*^{WT} and *Aire*^{KO} mice. The data are derived from at least 3 independent experiments (n = 3–4 mice per group and per experiment). **F** The expression of *Ccl20* and *Cxcl12* was measured by qPCR in purified mTEC^{hi} (EpCAM⁺UEA-1⁺Ly51$^{-/lo}$CD80^{hi}) from 6-week-old *Aire*^{WT} and *Aire*^{KO} mice. Bar graphs show ± SEM, $^{*}p < 0.05$, $^{**}p < 0.01$, $^{***}p < 0.001$, $^{****}p < 0.0001$ using unpaired Student's t test (**A, B, C, E**) and two-tailed Mann–Whitney test for (**F**)

cell modulation, as well as the ectoenzymes *Entpd1* (CD39) and *Nt5e* (CD73), implicated in target cell metabolic disruption, was reduced in CCR6⁺ T_{reg} of *Aire*^{KO} mice. A similar altered suppressive signature was also observed in CCR6⁺ T_{reg} purified from the thymus of 1-year-old *Aire*^{KO} mice (Fig. S2).

To further determine the impact of Aire on the functional properties of CCR6⁺ T_{reg}, we analyzed their gene expression profile by high-throughput RNA sequencing (Fig. 3B, C). Genes showing a significant variation ($p \le 0.05$) in gene expression between *Aire*^{WT} and *Aire*^{KO} CCR6⁺ T_{reg} with a fold change difference > 2 or < 0.5 were considered as up- and down-regulated, respectively. We identified a total of 2 634 upregulated genes reaching significance for 1060 of them (Cuffdiff $p < 0.05$) in *Aire*^{WT} CCR6⁺ T_{reg} as compared to their *Aire*^{KO} counterparts (Fig. 3B). Moreover, only 1 175 genes were downregulated with 301 of them reaching significance (Cuffdiff $p < 0.05$). Thus, the expression of *Aire* in the thymus upregulates three times more genes than it downregulates in recirculating CCR6⁺ T_{reg}. In accordance with the altered T_{reg} suppressive signature observed by qPCR (Fig. 3A), we found that *Il10, Gzmb, Fasl, Lag3, Entpd1* and *Nt5e* were downregulated in CCR6⁺ T_{reg} of *Aire*^{KO} mice (Fig. 3C and Table S1). Furthermore, the expression of *Prdm1* (Blimp-1), which characterizes effector Th-like T_{reg} [38] and the terminally differentiated markers *Klrg1* and

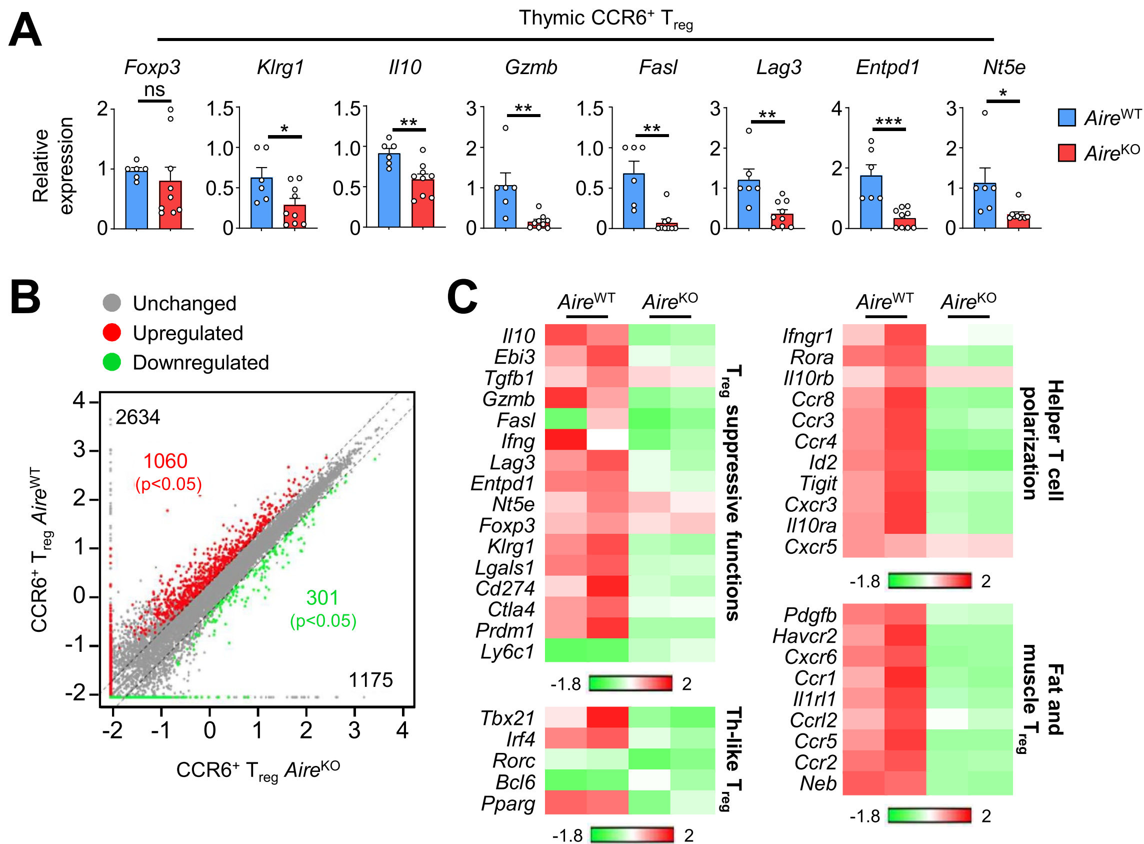

Fig. 3 The suppressive signature of recirculating CCR6+ T_{reg} is impaired in the thymus of $Aire^{KO}$ mice. **A** The expression level of *Foxp3, Klrg1, Il10, Gzmb, Fasl, Lag3, Entpd1 and Nt5e* was measured by qPCR in thymic CCR6+ T_{reg} from 6-week-old $Aire^{WT}$ ($n=6$) and $Aire^{KO}$ ($n=9$) mice. Bar graphs show mean ± SEM, *p < 0.05, **p < 0.01, ***p < 0.001 using two-tailed Mann–Whitney test. **B** Scatterplot representations of log10 gene expression levels (FPKM) in recirculating CCR6+ T_{reg} from $Aire^{WT}$ and $Aire^{KO}$ mice. For representation purposes, expression values of genes below 0.01 were assigned to 0.01. Genes with fold difference > 2 and *p*-adj < 0.05 were considered as up- or down-regulated genes (red and green dots, respectively). RNA-seq was performed on 2 independent biological replicates derived from two mice. **C** Heatmap of selected genes down-regulated in recirculating CCR6+ $Aire^{KO}$ T_{reg} (Fold Change > 2) compared to their CCR6+ $Aire^{WT}$ counterparts and involved in T_{reg} suppressive functions, Th–like T_{reg}, helper T cell polarization, fat and muscle T_{reg}. Two biological replicates are shown for each condition

Tigit [37, 39] was reduced in CCR6+ T_{reg} of $Aire^{KO}$ mice compared to their $Aire^{WT}$ counterparts. Strikingly, CCR6+ T_{reg} of $Aire^{KO}$ mice also expressed lower levels of several genes associated with their suppressive signature such as *Ctla4* and *Lgals1* (galectin-1) implicated respectively in dendritic cell modulation and target cell apoptosis [40, 41]. The expression of *Tbx21* and *Irf4*, encoding for transcription factors associated with Th1- and Th2-like T_{reg}, as well as *Pparg* and *Id2* genes associated with fat-resident effector T_{reg} [42] was also diminished. Accordingly, the expression of the chemokine receptors *Cxcr3* of Th1-like, *Ccr4* and *Ccr8* of Th2-like as well as *Ccr1* and *Ccr2* of fat-resident T_{reg} [43], implicated in effector T_{reg} migration to the inflammatory site, was reduced in CCR6+ $Aire^{KO}$ T_{reg}. Altogether, these results indicate that *Aire* expression is crucial for the effector and suppressive properties of recirculating CCR6+ T_{reg} in the thymus.

Recirculating CCR6+ T_{reg} from $Aire^{KO}$ mice fail to attenuate the severity of multiorgan autoimmunity

Because numbers and suppressive signature of recirculating CCR6+ T_{reg} were reduced in the thymus of $Aire^{KO}$ mice, we analyzed whether these defects would be also observed in the periphery. Blood and splenic CD4+Foxp3+ T_{reg} from 6-week- and 1-year-old $Aire^{KO}$ mice showed similar frequencies, numbers and expression levels of suppressive genes as compared to their $Aire^{WT}$ counterparts (Fig. S3). We next assessed the ability of peripheral and thymic CCR6+ T_{reg} from $Aire^{KO}$ mice to dampen the severity of multiorgan autoimmunity. To this end, CD4+CD25+ T_{reg}-depleted splenocytes from CD45.1 WT mice were transferred into $Rag2^{KO}$ lymphopenic recipients. Four weeks later, splenic T_{reg} or thymic CCR6+ T_{reg} purified from either $Aire^{WT}$ or

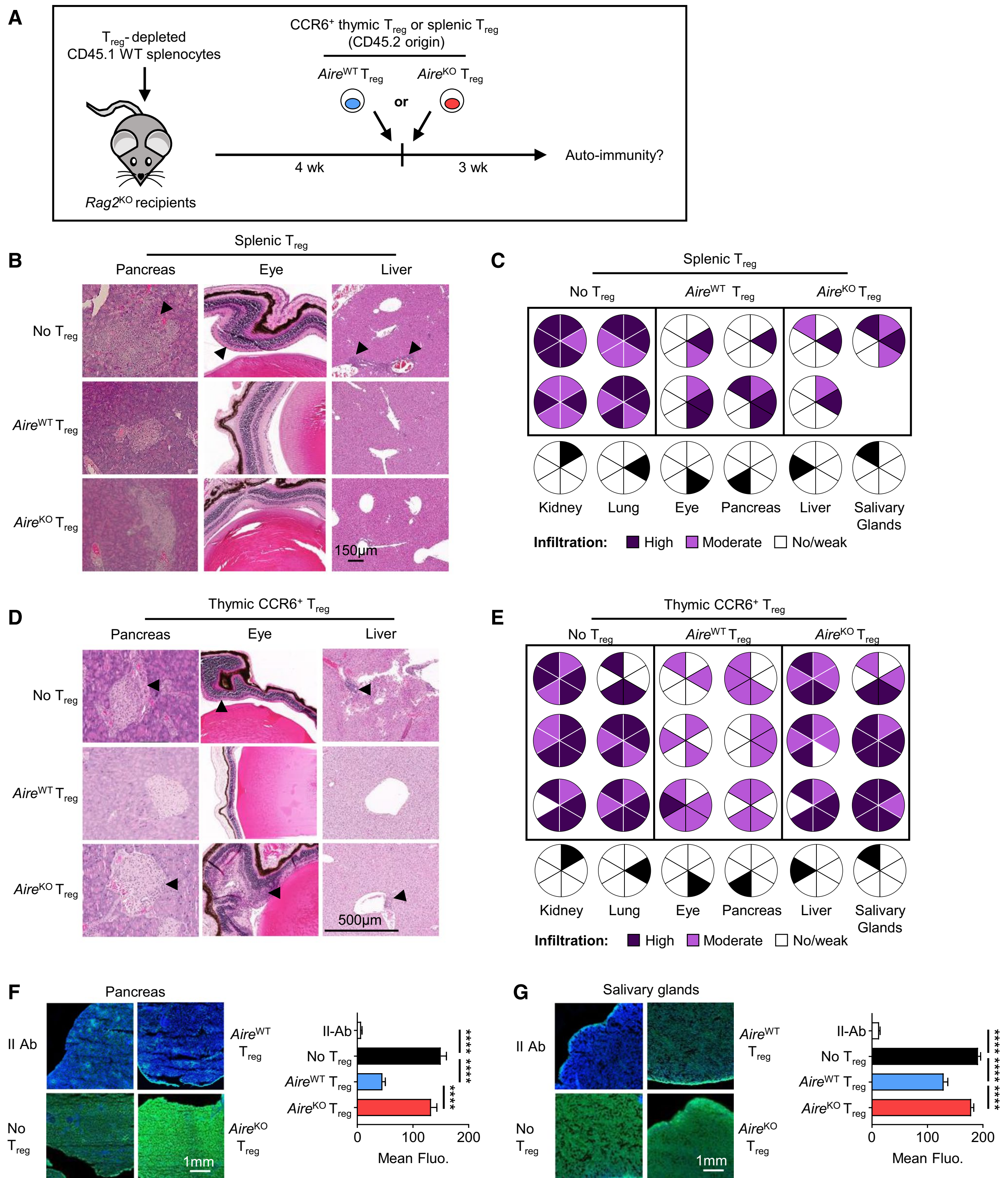

Aire^{KO} mice were adoptively transferred into these recipients (Figs. 4A and S4A). Signs of autoimmunity in peripheral tissues were visualized by histology and quantified by flow cytometry three weeks later. *Rag2*^{KO} mice that did not receive any T_{reg} were used as controls. Accordingly with the normal suppressive signature of splenic T_{reg} from *Aire*^{KO} mice (Fig. S3), *Rag2*^{KO} mice adoptively transferred with these cells show tissue infiltration levels similar to mice transferred with *Aire*^{WT} splenic T_{reg} (Fig. 4B, C). In marked contrast to mice that received *Aire*^{WT} thymic CCR6^{+} T_{reg},

◂**Fig. 4** The adoptive transfer of recirculating CCR6$^+$ T$_{reg}$ of the *Aire*^{KO} thymus fails to protect from multi-organ autoimmunity. **A** Experimental setup: *Rag2*^{KO} recipients were adoptively transferred with CD4$^+$CD25$^+$ T$_{reg}$-depleted CD45.1 WT splenocytes. Four weeks later, they were injected with splenic T$_{reg}$ or thymic CCR6$^+$ T$_{reg}$ derived from *Aire*^{WT} or *Aire*^{KO} mice. Three weeks after T$_{reg}$ adoptive transfer, peripheral tissues were examined for immune infiltration by histology and quantified by flow cytometry. *Rag2*^{KO} recipients injected only with CD4$^+$CD25$^+$ T$_{reg}$-depleted CD45.1 WT splenocytes were used as controls. **B-E** Representative photographies of peripheral tissue sections derived from mice transferred with splenic T$_{reg}$ (**B**) or thymic CCR6$^+$ T$_{reg}$ (**D**) and counterstained with hematoxylin/eosin. Diagrams represent organ infiltration levels by CD45.1 donor cells measured by flow cytometry upon splenic T$_{reg}$ (**C**) or thymic CCR6$^+$ T$_{reg}$ (**E**) transfer. Infiltration levels were normalized to the infiltration observed in controls. Dark and light violet in diagram represent high and low infiltrations. Each diagram represents one individual mouse. Scale bar, 150 µm for (**B**), 500 µm for (**D**). **F**, **G** Sera from mice transferred with CCR6$^+$ T$_{reg}$ were tested for the presence of autoantibodies (green) against pancreas (**F**) and salivary glands (**G**) of *Rag2*^{KO} mice. Nuclei were counterstained with DAPI (blue). Secondary antibodies (II Abs) alone were used as controls. Scale bar, 1 mm. Histograms show mean fluorescence intensity for each condition. Data are derived from 2 to 3 independent experiments ($n = 3$–5 mice per group and per experiment). Bar graphs show mean ± SEM, $^{****}p < 0.0001$ using unpaired Student's t test for (**F**, **G**)

mice adoptively transferred with thymic CCR6$^+$ T$_{reg}$ from *Aire*^{KO} mice failed to attenuate T-cell infiltration in several peripheral tissues despite similar numbers of CD45.2 donor Foxp3$^+$ T$_{reg}$ in lymph nodes (Fig. 4D, E and S4B, C). Examination of CD45.1 donor cell infiltration by flow cytometry revealed that 100% of *Rag2*^{KO} mice that received *Aire*^{KO} thymic CCR6$^+$ T$_{reg}$ showed a high infiltration level in the pancreas and salivary glands, 83% in eyes, 33% in the lung and liver as well as 16% in the kidney (Fig. 4E). In contrast, only 16% of *Rag2*^{KO} mice transferred with *Aire*^{WT} thymic CCR6$^+$ T$_{reg}$ showed a high infiltration in the liver. Furthermore, flow cytometry analysis showed that thymic CCR6$^+$ T$_{reg}$ of *Aire*^{KO} mice were unable to prevent the infiltration of CD45.1 CD4$^+$ and CD8$^+$ T cells in the pancreas and eyes as well as CD45.1 CD8$^+$ T cells in salivary glands (Fig. S4D). Finally, immunostaining of *Rag2*^{KO} tissue sections with sera from these mice revealed higher levels of autoantibodies against the pancreas and salivary glands in mice transferred with *Aire*^{KO} thymic CCR6$^+$ T$_{reg}$ than in mice injected with *Aire*^{WT} thymic CCR6$^+$ T$_{reg}$ (Fig. 4F, G). Thus, thymic CCR6$^+$ T$_{reg}$ of *Aire*^{KO} mice failed to attenuate the severity of multiorgan autoimmunity, demonstrating that their suppressive activity was impaired.

Aire expression in the thymic stroma controls the suppressive signature of recirculating CCR6$^+$ T$_{reg}$

Since *Aire* expression is not restricted to mTEC but was also found in thymic B cells [9], we then investigated its respective contribution in the stromal and hematopoietic compartments to control the recirculation and suppressive properties of CCR6$^+$ T$_{reg}$. To determine the role of Aire in hematopoietic cells, we generated BM chimeras by reconstituting lethally irradiated CD45.1/2 WT recipients with either CD45.2 *Aire*^{WT} or *Aire*^{KO} BM cells (Fig. S5A). Six weeks later, *Aire*^{KO} BM chimeras did not show major defects in total CD19$^+$B220$^+$ B cells, neither in the IgD$^-$ and IgD$^+$ B cell subsets, both described to express Aire [9] (Fig. S5B, C). Overall, frequencies and numbers of CD25$^+$ T$_{reg}$P, Foxp3^{lo} T$_{reg}$P, CCR6$^-$ and CCR6$^+$ mature CD25$^+$Foxp3$^+$ T$_{reg}$ were also normal (Fig. S5D, E). We next cell-sorted CCR6$^+$ T$_{reg}$ from the thymus of these BM chimeras and analyzed their suppressive signature. Recirculating T$_{reg}$ from both chimeras exhibited a similar expression of suppressive genes that was altered in CCR6$^+$ T$_{reg}$ of *Aire*^{KO} mice (Fig. S5F). Thus, *Aire* expression in thymic B cells is unlikely involved in T$_{reg}$ development, recirculation and suppressive signature.

We then analyzed whether *Aire* expression in stromal cells controls CCR6$^+$ T$_{reg}$ functional suppressive properties. To this end, we generated BM chimeras in which lethally irradiated CD45.2 *Aire*^{WT} or *Aire*^{KO} mice were reconstituted with CD45.1 Foxp3^{eGFP} BM cells (Fig. 5A). Six weeks later, similar numbers of CD4$^+$ SP thymocytes of CD45.1 donor origin were observed in *Aire*^{WT} and *Aire*^{KO} recipients (Fig. 5B). Although numbers of CD25$^+$ T$_{reg}$P and Foxp3^{lo} T$_{reg}$P were also similar in both groups, frequencies and numbers of mature CD25$^+$Foxp3$^+$ T$_{reg}$ were specifically reduced in *Aire*^{KO} chimeras (Fig. 5C). This defect was attributable to diminished frequencies and numbers of CCR6$^+$ T$_{reg}$ (Fig. 5D). Recirculating CCR6$^+$ mature CD25$^+$Foxp3$^+$ T$_{reg}$ of CD45.1 origin were then cell-sorted from the thymus of both chimeras and analyzed for the expression of several genes associated with T$_{reg}$ effector functions. Whereas *Foxp3* level was normal, the expression of *Klrg1, Il10*, *Tgfb1*, *Gzmb*, *Fasl*, *Lag3*, *Entpd1* and *Nt5e* was reduced in *Aire*^{KO} chimeras as compared to control chimeras (Fig. 5E). Altogether, these results show that whereas *Aire* in hematopoietic cells is dispensable, its specific expression in stromal cells controls both recirculation and suppressive properties of CCR6$^+$ T$_{reg}$.

Antigen-specific restimulation of recirculating T$_{reg}$ by Aire$^+$ mTEC

To further decipher the impact of *Aire*-expressing mTEC in the suppressive signature of recirculating T$_{reg}$, we used an in vitro co-culture setup of peripheral T$_{reg}$ and mTEC purified from *Aire*^{WT} or *Aire*^{KO} mice. Compared with *Aire*^{WT} splenic T$_{reg}$ co-cultured with *Aire*^{WT} mTEC, the expression of *Tgfb1*, *Gzmb*, *Fasl*, *Entpd1* and *Nt5e* was reduced in *Aire*^{WT} splenic T$_{reg}$ co-cultured with *Aire*^{KO} mTEC (Fig. 6A). Moreover, *Aire*^{KO} splenic T$_{reg}$ co-cultured with *Aire*^{WT} mTEC upregulated the expression of these genes

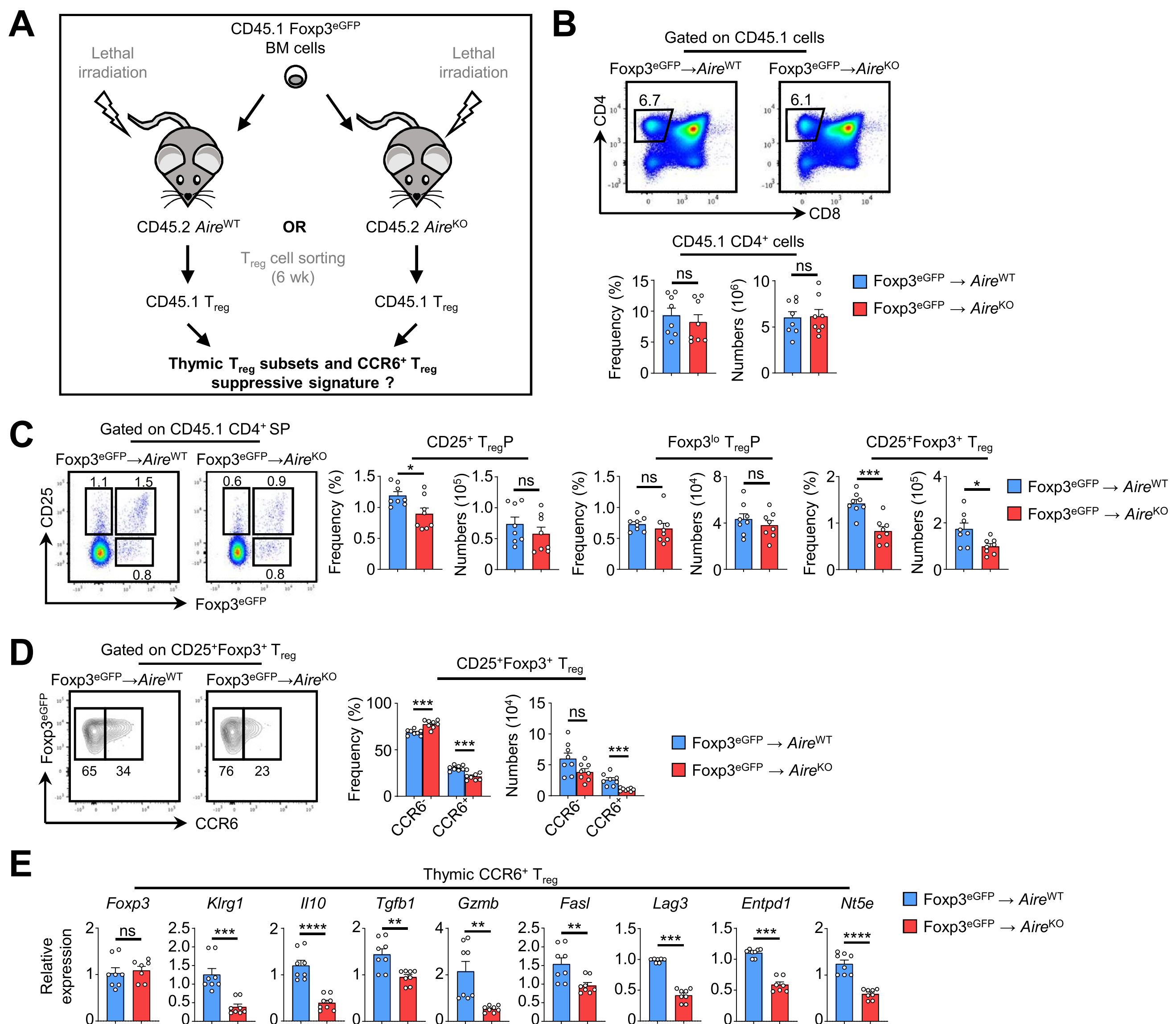

Fig. 5 *Aire* deficiency in the thymic stroma impairs the recirculation and the suppressive signature of CCR6$^+$ T$_{reg}$. **A** Experimental setup: lethally irradiated CD45.2 *Aire*^{WT} or *Aire*^{KO} recipients were reconstituted with BM cells from CD45.1 Foxp3^{eGFP} mice. Six weeks later, thymic T$_{reg}$ subsets of CD45.1 origin were analyzed by flow cytometry. CCR6$^+$ T$_{reg}$ were cell-sorted to measure the expression levels of genes associated with their suppressive functions. **B** Flow cytometry profiles, frequencies and numbers of CD4$^+$ SP thymocytes of CD45.1 origin in the thymus of BM chimeric mice. **C**, **D** Flow cytometry profiles and numbers of CD25$^+$ T$_{reg}$P, Foxp3^{lo} T$_{reg}$P and total CD25$^+$Foxp3$^+$ cells (**C**) as well as of CCR6$^-$ and CCR6$^+$ cells in CD25$^+$Foxp3$^+$ T$_{reg}$ (**D**) of CD45.1 origin in the thymus of BM chimeras. Data are derived from 2 independent experiments ($n=4$ mice per group and per experiment). **E** The expression level of *Foxp3, Klrg1, Il10, Tgfb1, Gzmb, Fasl, Lag3, Entpd1* and *Nt5e* was measured by qPCR in purified CCR6$^+$CD25$^+$Foxp3$^+$ T$_{reg}$ from CD45.1 Foxp3^{eGFP}→*Aire*^{WT} ($n=8$) and CD45.1 Foxp3^{eGFP}→*Aire*^{KO} ($n=9$) chimeras. Data are derived from 2 independent experiments (n = 4–5 mice per group and per experiment). Bar graphs show mean ± SEM, $*p<0.05$, $**p<0.01$, $***p<0.001$, $****p<0.0001$ using unpaired Student's *t* test for (**B-D**) and two-tailed Mann–Whitney test for (**E**)

in contrast to *Aire*^{KO} splenic T$_{reg}$ co-cultured with *Aire*^{KO} mTEC. Thus, as compared to their *Aire*^{WT} counterparts, *Aire*^{KO} mTEC failed to enhance suppressive signatures of both *Aire*^{WT} and *Aire*^{KO} splenic T$_{reg}$.

We then analyzed the in vivo effect of the *Aire*^{KO} thymic stroma in regulating the suppressive signature of peripheral WT T$_{reg}$. To this end, splenic T$_{reg}$ purified from CD45.1 Foxp3^{eGFP} congenic mice were adoptively transferred into either *Aire*^{WT} or *Aire*^{KO} recipients (Fig. 6B). One week later, we observed reduced frequencies and numbers of donor CD45.1 Foxp3^{eGFP} T$_{reg}$ in the thymus of *Aire*^{KO} mice as compared to *Aire*^{WT} mice (Fig. 6C). Moreover, the remaining donor Foxp3^{eGFP} T$_{reg}$ that recirculated back to the thymus exhibited an impaired suppressive signature (Fig. 6D).

These results not only confirm that Aire favors the recirculation of peripheral T_{reg} in the thymus but also highlight its key role in enhancing their suppressive properties.

Thus, we made the hypothesis that recirculating T_{reg} could be restimulated by $Aire^+$ mTEC. To test this, WT thymic sections were first stained for Aire, Foxp3 and CD73, the latter being a reliable marker of recirculating T_{reg} [1, 44]. Of note, anti-CCR6 antibody was not used in this experiment because it failed to give any signal in our hands. Interestingly, we observed that both developing $CD73^-$ and recirculating $CD73^+$ T_{reg} were found in close proximity to $Aire^+$ mTEC (Fig. 6E). These results suggest that recirculating T_{reg} could be restimulated by establishing antigen-specific contacts with $Aire^+$ mTEC. To test this hypothesis, splenic OTII T_{reg} from Rip-mOVA x OTII mice were co-cultured with $OVA_{323-339}$-loaded $Aire^{het}$ ($Aire^{eGFP/WT}$) or $Aire^{KO}$ ($Aire^{eGFP/eGFP}$) $mTEC^{hi}$ (Fig. S6). When compared with unstimulated OVA-specific T_{reg}, $Aire^{KO}$ $mTEC^{hi}$ were able to activate OTII T_{reg} but to a lesser extent than $Aire^{het}$ $mTEC^{hi}$ (Fig. 6F). These results demonstrate that $Aire^+$ mTEC can stimulate peripheral T_{reg} in an antigen-specific manner and this ability is impaired in the absence of Aire. Furthermore, as compared to OTII T_{reg} co-cultured with $Aire^{het}$ $mTEC^{hi}$, the expression of *Il10*, *Tgfb1*, *Gzmb*, *Fasl*, *Lag3*, *Entpd1* and *Nt5e* was reduced in OTII T_{reg} co-cultured with $Aire^{KO}$ $mTEC^{hi}$ (Fig. 6G), indicating that this antigen-specific restimulation is much less efficient. We thus analyzed MHCII expression in mTEC from $Aire^{KO}$ mice. In accordance with a previous study [45] and the pro-apoptotic role of Aire [46], we found increased frequencies of $MHCII^+$ mTEC in these mice (Fig. S7A). We then made the hypothesis that costimulatory signals may be implicated in the phenotype observed. Two ligands of the Tumor Necrosis Factor Superfamily (TNFSF) have been described to be constitutively expressed by mTEC and participate in thymic T_{reg} development [47]. Interestingly, we found that $mTEC^{hi}$ expressed reduced levels of *Tnfsf4* (OX40L, $Aire^{WT}$: 2.32 FPKM vs $Aire^{KO}$: 0.37) and *Tnfsf18* (GITRL, $Aire^{WT}$: 2.92 vs $Aire^{KO}$: 0.81) in $Aire^{KO}$ mice (Fig. S7B). This result was also confirmed at the protein level by flow cytometry (Fig. S7C). These observations are consistent with the reduced cellularity of $Foxp3^{lo}$ $T_{reg}P$ and $CD25^+Foxp3^+$ T_{reg} in $Aire^{KO}$ mice (Fig. 2A–C). Further investigations are needed to decipher the role of these two TNFSF ligands in the biology of recirculating T_{reg} in the thymus. Altogether, our data reveal that $Aire^+$ mTEC, through antigen-specific restimulation, are responsible for the strong suppressive signature of recirculating T_{reg}.

Discussion

Our study demonstrates that Aire expression by mTEC promotes the suppressive properties of recirculating $CCR6^+$ T_{reg} independently of the dynamic remodeling of the medullary 3D organization, where recirculating T_{reg} reside. We previously described that the medulla of 6-week-old young adult mice is complex with a large central compartment surrounded by hundreds of individual islets [32]. Nevertheless, determining whether this topology varies throughout life and whether Aire is implicated remained open issues. Interestingly, we found that 9-day- and 6-week-old WT mice show ~ 1000 and ~ 400 medullary islets, respectively. Given that individual islets arise from a single progenitor [48], these observations suggest that during thymic development, they grow and fuse together, leading to a reduced number of islets in young adult mice as compared to neonates. In 1-year-old mice, the number of medullary islets increases to reach ~ 1000 islets, as observed in neonates. Considering that the medulla topology is governed by crosstalk with autoreactive $CD4^+$ thymocytes [32, 49–52], the high islet number observed in aged mice could be due to a suboptimal cellular crosstalk due to reduced cellularity of $CD4^+$ thymocytes linked to age-related thymic involution. Although Aire plays multiple roles in T-cell tolerance induction [34], our results show that it does not shape the 3D organization of the thymic medulla. This is consistent with the fact that the clonal deletion of autoreactive $CD4^+$ thymocytes is impaired in $Aire^{KO}$ mice [45, 53], which consequently leads to an effective medulla organization.

Several studies have shown that mTEC are implicated in $Foxp3^+$ T_{reg} development [54–56]. Nevertheless, the specific role of Aire in thymic T_{reg} heterogeneity throughout life remained to be defined. Interestingly, we found that Aire controls the cellularity of $Foxp3^{lo}$ $T_{reg}P$ and mature $CD25^+Foxp3^+$ T_{reg} in 5-day-, 6-week- and 1-year-old mice. This is illustrated by decreased numbers of $Foxp3^{lo}$ $T_{reg}P$ and $CD25^+Foxp3^+$ T_{reg} in $Aire^{KO}$ mice, which could not be due to impaired medulla organization since no defect was observed at this level. Given that $CD25^+$ $T_{reg}P$ and $Foxp3^{lo}$ $T_{reg}P$ show distinct developmental pathways that give rise to $CD25^+Foxp3^+$ T_{reg} with non-overlapping regulatory activities [1], our results provide new insights in the role of Aire in the emergence of $Foxp3^{lo}$ $T_{reg}P$. Furthermore, Aire regulates the pool of recirculating $CCR6^+$ T_{reg} throughout life. Interestingly, $CCR6^+$ T_{reg} from $Aire^{KO}$ mice expressed reduced levels of several genes associated with their polarization and suppressive functions. Importantly, they express normal levels of *Foxp3*, indicating that they remain engaged in the T_{reg} cell lineage. In accordance with the defective suppressive signature of $CCR6^+$ T_{reg} from $Aire^{KO}$ mice, we found that the adoptive transfer of these cells failed to attenuate the

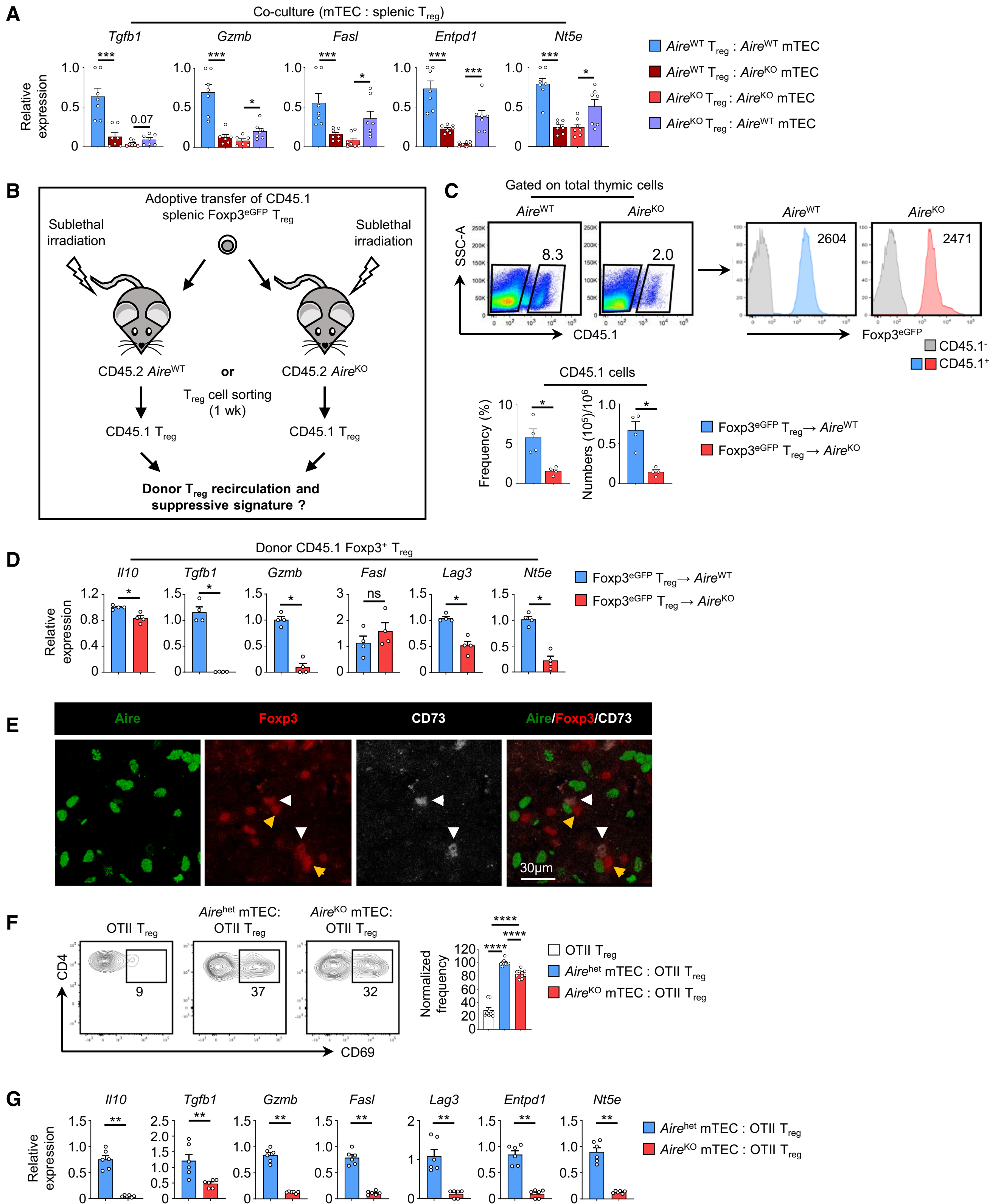

severity of multiorgan autoimmunity. In contrast to their thymic counterparts, splenic T_{reg} of *Aire*^{KO} mice show a protection similar to *Aire*^{WT} splenic T_{reg}, consistently with their normal suppressive signature. Altogether, these results indicate that Aire is crucial for the suppressive functions of recirculating CCR6^{+} T_{reg} in the thymus.

◂**Fig. 6** Aire$^+$ mTEC control the activation and suppressive signature of recirculating T_{reg} through antigen-dependent contact. **A** The expression level of *Tgfb1, Gzmb, Fasl, Entpd1* and *Nt5e* was measured by qPCR in splenic T_{reg} from *Aire*^{WT} or *Aire*^{KO} mice co-cultured with *Aire*^{WT} or *Aire*^{KO} mTEC. Data are derived from 2 independent experiments. **B** Experimental setup: purified splenic T_{reg} from CD45.1 Foxp3^{eGFP} mice were adoptively transferred *i.v.* into sublethally irradiated CD45.2 *Aire*^{WT} or *Aire*^{KO} recipients. Adoptively transferred CD45.1 Foxp3^{eGFP} T_{reg} were cell-sorted from the thymus of recipient mice one week later and their suppressive signature was analyzed by qPCR. **C** Flow cytometry profiles, frequencies and numbers of CD45.1 Foxp3^{eGFP} donor T_{reg} observed in the thymus of CD45.2 *Aire*^{WT} or *Aire*^{KO} recipients. **D** The expression level of *Il10, Tgfb1, Gzmb, Fasl, Lag3* and *Nt5e* was measured by qPCR in CD45.1 Foxp3^{eGFP} donor T_{reg} transferred into *Aire*^{WT} ($n=4$) or *Aire*^{KO} ($n=4$) recipients. **E** Representative images of WT thymic sections stained for Aire (green), Foxp3 (red) and CD73 (white). Yellow and white arrowheads denote developing CD73$^-$ and recirculating CD73$^+$ T_{reg}, respectively. Scale bar, 30 µm. **F** Flow cytometry profiles of CD69 activation of splenic OTII T_{reg} from Rip-mOVA x OTII x *Rag2*^{KO} mice co-cultured with $OVA_{323-339}$-loaded *Aire*^{het} (*Aire*$^{eGFP/WT}$) or *Aire*^{KO} (*Aire*$^{eGFP/eGFP}$) mTEC^{hi} after 24 h later. The histogram shows the frequencies of CD69$^+$ T_{reg} normalized to the activation of OTII T_{reg} co-cultured with *Aire*^{het} mTEC^{hi}. **G** The expression level of *Il10, Tgfb1, Gzmb, Fasl, Lag3, Entpd1* and *Nt5e* was measured by qPCR in splenic OTII T_{reg} from Rip-mOVA x OTII x *Rag2*^{KO} mice co-cultured with $OVA_{323-339}$-loaded *Aire*^{het} (*Aire*$^{eGFP/WT}$; $n=6$) or *Aire*^{KO} (*Aire*$^{eGFP/eGFP}$; $n=6$) mTEC^{hi}. Data are derived from 2 independent experiments. Bar graphs show mean ± SEM, $*p<0.05$, $**p<0.01$, $***p<0.001$ and $****p<0.0001$ using two-tailed Mann–Whitney test for (**A**, **C**, **D**, **F**, **G**)

Although Aire is expressed by a subset of recirculating thymic B cells [9], we found that its absence in hematopoietic cells had no impact neither in T_{reg} development nor in CCR6$^+$ T_{reg} recirculation and suppressive signature. Considering the weak expression of *Aire* in thymic B cells as compared to mTEC, it is not surprising that *Aire* deficiency in hematopoietic cells does not control the cellularity and suppressive signature of CCR6$^+$ T_{reg}. In marked contrast, beyond controlling the recirculation of CCR6$^+$ T_{reg}, BM chimeras in *Aire*^{KO} recipients revealed that *Aire* expression in stromal cells is responsible for their highly suppressive phenotype.

Interestingly, recirculating Foxp3$^+$ T_{reg} were observed in close proximity to Aire$^+$ mTEC, similarly to developing Foxp3$^+$ T_{reg}. The reduced expression of *Ccl20* and *Cxcl12*, likely responsible for the lower amount of recirculating T_{reg} in these mice [5, 8], could contribute to a lesser stimulation of recirculating T_{reg} by mTEC. However, in vitro co-culture experiments suggest that defective chemoattraction is unlikely responsible for the phenotype observed in *Aire*^{KO} mice. Furthermore, in vitro co-culture assays revealed that Aire$^+$ mTEC were capable to activate peripheral T_{reg} in an antigen-specific manner. Our results suggest that peripheral T_{reg} could regulate de novo T_{reg} development not only by competing for IL-2 [5, 57] but also for the cognate self-antigen. In the absence of Aire, in vitro co-culture assays and in vivo adoptive transfer experiments demonstrate that recirculating T_{reg} activation and suppressive signature were altered. Therefore, our results unravel that Aire$^+$ mTEC control the activated and differentiated phenotype of recirculating T_{reg} upon their entry into the thymus. A possible explanation could be that Aire controls co-stimulation signals that are responsible for maintaining the effector phenotype of recirculating T_{reg}. In addition, Aire could also modulate indirectly CCR6$^+$ T_{reg} suppressive properties through other mechanisms such as the medullary positioning of XCR1$^+$ type 1 conventional dendritic cells by controlling the production of the chemokine XCL1 [11]. Moreover, further investigations are required to determine the fate of CCR6$^+$ T_{reg} in the thymic medulla. Three possibilities can be envisaged: CCR6$^+$ T_{reg} (1) become long-term resident cells, (2) migrate back to the periphery or (3) die by apoptosis.

This study ameliorates our understanding on recirculating T_{reg} in the thymus, which remain poorly described to date. In summary, it identifies that Aire controls the suppressive properties of recirculating CCR6$^+$ T_{reg} in the thymus. It also assigns a new role for Aire in conferring to mTEC the aptitude to restimulate recirculating T_{reg}. Thus, this study furthers our understanding on the mechanisms allowing recirculating T_{reg} to fine-tune de novo T_{reg} production. Finally, our results are expected to contribute to a better understanding of T_{reg} deficiencies observed in the human pathology APECED.

Supplementary Information The online version contains supplementary material available at https://doi.org/10.1007/s00018-022-04328-9.

Acknowledgements We are grateful to Georg Holländer (University of Basel, Switzerland) and Bernard Malissen (CIML, Marseille, France) for providing us *Aire*^{KO} and Foxp3^{eGFP} mice, respectively. We thank the CIML flow cytometry, histology, PICSL imaging facility of the CIML (ImagImm) and animal facility platforms for technical support. We thank Cloé Zamit (CIML, France) for help with mouse genotyping.

Author contributions JC, AB, JCS, LC and MI conducted the experiments, analyzed and interpreted the data. MG and AS analyzed the data. JC, AB, JCS and MI wrote the manuscript. MI initiated, supervised and conceived the study.

Funding This work was supported by institutional grants from INSERM, CNRS and Aix-Marseille Université. The Immune Tolerance and T-Cell Differentiation laboratory received funding from the ARC Foundation (PJA20171206491 to M.I.), CoPoC-proof of concept (MAT-PI-17326-A-01 to M.I.), a prematuration grant from A*MIDEX, a French "Investissements d'avenir" program (LTalpha-Treg to M.I.) and Agence Nationale de la Recherche (grant ANR-19-CE18-0021–01, *RANKLthym* to M.I.). We also acknowledge financial support from France Bio Imaging (ANR-10-INBS-04–01) and France Génomique national infrastructure, funded as part of the "Investissements d'Avenir" program managed by the ANR (ANR-10-INBS-0009). J.C. and A.B. were supported by a PhD fellowship from the Ministère de l'Enseignement Supérieur et de la Recherche et de l'Innovation (MESRI).

Data availability All data generated or analyzed during this study are included in this published article and its supplementary information files. The dataset generated in this study are available in the Gene Expression Omnibus (GEO) database under accession number GSE188419.

Code availability Not applicable.

Declarations

Conflict of interest The authors declare that they have no conflict of interest.

Ethical approval All experiments were done in accordance with National and European laws for laboratory animal welfare (EEC Council Directive 2010/63/UE) and the Marseille Ethical Committee for Animal experimentation.

Consent to participate Not applicable.

Consent to publication Not applicable.

References

1. Owen DL, Mahmud SA, Sjaastad LE, Williams JB, Spanier JA, Simeonov DR et al (2019) Thymic regulatory T cells arise via two distinct developmental programs. Nat Immunol 20(2):195–205
2. Lio CW, Hsieh CS (2008) A two-step process for thymic regulatory T cell development. Immunity 28(1):100–111
3. Santamaria JC, Borelli A, Irla M (2021) Regulatory T cell heterogeneity in the thymus: impact on their functional activities. Front Immunol 12:643153
4. Marshall D, Sinclair C, Tung S, Seddon B (2014) Differential requirement for IL-2 and IL-15 during bifurcated development of thymic regulatory T cells. J Immunol 193(11):5525–5533
5. Thiault N, Darrigues J, Adoue V, Gros M, Binet B, Perals C et al (2015) Peripheral regulatory T lymphocytes recirculating to the thymus suppress the development of their precursors. Nat Immunol 16:628–634
6. Cowan JE, McCarthy NI, Anderson G (2016) CCR7 controls thymus recirculation, but not production and emigration, of Foxp3(+) T cells. Cell Rep 14(5):1041–1048
7. Yang E, Zou T, Leichner TM, Zhang SL, Kambayashi T (2014) Both retention and recirculation contribute to long-lived regulatory T-cell accumulation in the thymus. Eur J Immunol 44(9):2712–2720
8. Cowan JE, Baik S, McCarthy NI, Parnell SM, White AJ, Jenkinson WE et al (2018) Aire controls the recirculation of murine Foxp3(+) regulatory T-cells back to the thymus. Eur J Immunol 48(5):844–854
9. Yamano T, Nedjic J, Hinterberger M, Steinert M, Koser S, Pinto S et al (2015) Thymic B cells are licensed to present self antigens for central T cell tolerance induction. Immunity 42:1048–1061
10. Aricha R, Feferman T, Scott HS, Souroujon MC, Berrih-Aknin S, Fuchs S (2011) The susceptibility of Aire(-/-) mice to experimental myasthenia gravis involves alterations in regulatory T cells. J Autoimmun 36(1):16–24
11. Lei Y, Ripen AM, Ishimaru N, Ohigashi I, Nagasawa T, Jeker LT et al (2011) Aire-dependent production of XCL1 mediates medullary accumulation of thymic dendritic cells and contributes to regulatory T cell development. J Exp Med 208(2):383–394
12. Malchow S, Leventhal DS, Lee V, Nishi S, Socci ND, Savage PA (2016) Aire enforces immune tolerance by directing autoreactive T cells into the regulatory T cell lineage. Immunity 44(5):1102–1113
13. Yang S, Fujikado N, Kolodin D, Benoist C, Mathis D (2015) Immune tolerance. Regulatory T cells generated early in life play a distinct role in maintaining self-tolerance. Science 348(6234):589–594
14. Anderson MS, Venanzi ES, Klein L, Chen Z, Berzins SP, Turley SJ et al (2002) Projection of an immunological self shadow within the thymus by the aire protein. Science 298(5597):1395–1401
15. Jiang W, Anderson MS, Bronson R, Mathis D, Benoist C (2005) Modifier loci condition autoimmunity provoked by Aire deficiency. J Exp Med 202(6):805–815
16. Kuroda N, Mitani T, Takeda N, Ishimaru N, Arakaki R, Hayashi Y et al (2005) Development of autoimmunity against transcriptionally unrepressed target antigen in the thymus of Aire-deficient mice. J Immunol 174(4):1862–1870
17. Ramsey C, Winqvist O, Puhakka L, Halonen M, Moro A, Kämpe O et al (2002) Aire deficient mice develop multiple features of APECED phenotype and show altered immune response. Hum Mol Genet 11(4):397–409
18. Consortium. F-GA (1997) An autoimmune disease, APECED, caused by mutations in a novel gene featuring two PHD-type zinc-finger domains. Nat Genet 17(4):399–403
19. Nagamine K, Peterson P, Scott HS, Kudoh J, Minoshima S, Heino M et al (1997) Positional cloning of the APECED gene. Nat Genet 17(4):393–398
20. Ryan KR, Lawson CA, Lorenzi AR, Arkwright PD, Isaacs JD, Lilic D (2005) CD4+CD25+ T-regulatory cells are decreased in patients with autoimmune polyendocrinopathy candidiasis ectodermal dystrophy. J Allergy Clin Immunol 116(5):1158–1159
21. Kekäläinen E, Tuovinen H, Joensuu J, Gylling M, Franssila R, Pöntynen N et al (2007) A defect of regulatory T cells in patients with autoimmune polyendocrinopathy-candidiasis-ectodermal dystrophy. J Immunol 178(2):1208–1215
22. Laakso SM, Laurinolli TT, Rossi LH, Lehtoviita A, Sairanen H, Perheentupa J et al (2010) Regulatory T cell defect in APECED patients is associated with loss of naive FOXP3(+) precursors and impaired activated population. J Autoimmun 35(4):351–357
23. Sansom SN, Shikama-Dorn N, Zhanybekova S, Nusspaumer G, Macaulay IC, Deadman ME, et al (2014) Population and single-cell genomics reveal the aire dependency, relief from polycomb silencing, and distribution of self-antigen expression in thymic epithelia. Genome Res 24(12):1918–1931
24. Shinkai Y, Rathbun G, Lam KP, Oltz EM, Stewart V, Mendelsohn M et al (1992) RAG-2-deficient mice lack mature lymphocytes owing to inability to initiate V(D)J rearrangement. Cell 68(5):855–867
25. Wang Y, Kissenpfennig A, Mingueneau M, Richelme S, Perrin P, Chevrier S et al (2008) Th2 lymphoproliferative disorder of LatY136F mutant mice unfolds independently of TCR-MHC engagement and is insensitive to the action of Foxp3+ regulatory T cells. J Immunol 180(3):1565–1575
26. Barnden MJ, Allison J, Heath WR, Carbone FR (1998) Defective TCR expression in transgenic mice constructed using cDNA-based alpha- and beta-chain genes under the control of heterologous regulatory elements. Immunol Cell Biol 76(1):34–40
27. Kurts C, Heath WR, Carbone FR, Allison J, Miller JF, Kosaka H (1996) Constitutive class I-restricted exogenous presentation of self antigens in vivo. J Exp Med 184(3):923–930
28. Kim D, Pertea G, Trapnell C, Pimentel H, Kelley R, Salzberg SL (2013) TopHat2: accurate alignment of transcriptomes in the presence of insertions, deletions and gene fusions. Genome Biol 14(4):R36

29. Trapnell C, Williams BA, Pertea G, Mortazavi A, Kwan G, van Baren MJ et al (2010) Transcript assembly and quantification by RNA-Seq reveals unannotated transcripts and isoform switching during cell differentiation. Nat Biotechnol 28(5):511–515
30. Trapnell C, Hendrickson DG, Sauvageau M, Goff L, Rinn JL, Pachter L (2013) Differential analysis of gene regulation at transcript resolution with RNA-seq. Nat Biotechnol 31(1):46–53
31. Pavlidis P, Noble WS (2003) Matrix2png: a utility for visualizing matrix data. Bioinformatics 19(2):295–296
32. Irla M, Guenot J, Sealy G, Reith W, Imhof BA, Serge A (2013) Three-dimensional visualization of the mouse thymus organization in health and immunodeficiency. J Immunol 190(2):586–596
33. Serge A, Bailly AL, Aurrand-Lions M, Imhof BA, Irla M (2015) For3D: full organ reconstruction in 3D, an automatized tool for deciphering the complexity of lymphoid organs. J Immunol Methods 424:32–42
34. Perniola R (2018) Twenty Years of AIRE Front Immunol 9:98
35. Klug DB, Carter C, Crouch E, Roop D, Conti CJ, Richie ER (1998) Interdependence of cortical thymic epithelial cell differentiation and T-lineage commitment. Proc Natl Acad Sci USA 95(20):11822–11827
36. Fontenot JD, Dooley JL, Farr AG, Rudensky AY (2005) Developmental regulation of Foxp3 expression during ontogeny. J Exp Med 202(7):901–906
37. Cheng G, Yuan X, Tsai MS, Podack ER, Yu A, Malek TR (2012) IL-2 receptor signaling is essential for the development of Klrg1+ terminally differentiated T regulatory cells. J Immunol 189(4):1780–1791
38. Cretney E, Kallies A, Nutt SL (2013) Differentiation and function of Foxp3(+) effector regulatory T cells. Trends Immunol 34(2):74–80
39. Joller N, Lozano E, Burkett PR, Patel B, Xiao S, Zhu C et al (2014) Treg cells expressing the coinhibitory molecule TIGIT selectively inhibit proinflammatory Th1 and Th17 cell responses. Immunity 40(4):569–581
40. Fallarino F, Grohmann U, Hwang KW, Orabona C, Vacca C, Bianchi R et al (2003) Modulation of tryptophan catabolism by regulatory T cells. Nat Immunol 4(12):1206–1212
41. Garín MI, Chu CC, Golshayan D, Cernuda-Morollón E, Wait R, Lechler RI (2007) Galectin-1: a key effector of regulation mediated by CD4+CD25+ T cells. Blood 109(5):2058–2065
42. Frias AB Jr, Hyzny EJ, Buechel HM, Beppu LY, Xie B, Jurczak MJ et al (2019) The transcriptional regulator Id2 is critical for adipose-resident regulatory T cell differentiation, survival, and function. J Immunol 203(3):658–664
43. Sawant DV, Vignali DA (2014) Once a Treg, always a Treg? Immunol Rev 259(1):173–191
44. Peligero-Cruz C, Givony T, Sebé-Pedrós A, Dobeš J, Kadouri N, Nevo S et al (2020) IL18 signaling promotes homing of mature Tregs into the thymus. Elife 9:e58213
45. Anderson MS, Venanzi ES, Chen Z, Berzins SP, Benoist C, Mathis D (2005) The cellular mechanism of Aire control of T cell tolerance. Immunity 23(2):227–239
46. Gray D, Abramson J, Benoist C, Mathis D (2007) Proliferative arrest and rapid turnover of thymic epithelial cells expressing Aire. J Exp Med 204(11):2521–2528
47. Mahmud SA, Manlove LS, Schmitz HM, Xing Y, Wang Y, Owen DL et al (2014) Costimulation via the tumor-necrosis factor receptor superfamily couples TCR signal strength to the thymic differentiation of regulatory T cells. Nat Immunol 15(5):473–481
48. Rodewald HR, Paul S, Haller C, Bluethmann H, Blum C (2001) Thymus medulla consisting of epithelial islets each derived from a single progenitor. Nature 414(6865):763–768
49. Irla M, Guerri L, Guenot J, Serge A, Lantz O, Liston A et al (2012) Antigen recognition by autoreactive cd4(+) thymocytes drives homeostasis of the thymic medulla. PLoS ONE 7(12):e52591
50. Lopes N, Serge A, Ferrier P, Irla M (2015) Thymic crosstalk coordinates medulla organization and T-cell tolerance induction. Front Immunol 6:365
51. Lopes N, Boucherit N, Santamaria JC, Provin N, Charaix J, Ferrier P, et al (2022) Thymocytes trigger self-antigen-controlling pathways in immature medullary thymic epithelial stages. Elife 11:e69982
52. Borelli A, Irla M (2021) Lymphotoxin: from the physiology to the regeneration of the thymic function. Cell Death Differ 28(8):2305–2314
53. Liston A, Lesage S, Wilson J, Peltonen L, Goodnow CC (2003) Aire regulates negative selection of organ-specific T cells. Nat Immunol 4(4):350–354
54. Cowan JE, Parnell SM, Nakamura K, Caamano JH, Lane PJ, Jenkinson EJ et al (2013) The thymic medulla is required for Foxp3+ regulatory but not conventional CD4+ thymocyte development. J Exp Med 210(4):675–681
55. Aschenbrenner K, D'Cruz LM, Vollmann EH, Hinterberger M, Emmerich J, Swee LK et al (2007) Selection of Foxp3+ regulatory T cells specific for self antigen expressed and presented by Aire+ medullary thymic epithelial cells. Nat Immunol 8(4):351–358
56. Malchow S, Leventhal DS, Nishi S, Fischer BI, Shen L, Paner GP et al (2013) Aire-dependent thymic development of tumor-associated regulatory T cells. Science 339(6124):1219–1224
57. Weist BM, Kurd N, Boussier J, Chan SW, Robey EA (2015) Thymic regulatory T cell niche size is dictated by limiting IL-2 from antigen-bearing dendritic cells and feedback competition. Nat Immunol 16(6):635–641

Publisher's Note Springer Nature remains neutral with regard to jurisdictional claims in published maps and institutional affiliations.